Proceedings of ISFOG 2025
5TH INTERNATIONAL SYMPOSIUM ON
FRONTIERS IN OFFSHORE GEOTECHNICS
Nantes, France | June 9-13 2025

ISBN 978-2-85782-758-0

Seismic Vulnerability of 10 MW TLP Floating Wind Turbines in Intermediate Water Depth

M. James
Indian Institute of Technology Bhubaneswar, Odisha, India
S. Haldar*
Indian Institute of Technology Bhubaneswar, Odisha, India
S. Bhattacharya
University of Surrey, Guildford, United Kingdom
**sumanta@iitbbs.ac.in (corresponding author)*

ABSTRACT: The expansion of offshore wind farms into earthquake-prone regions necessitates careful consideration of their seismic performance. Previous studies have focused on the seismic design of fixed wind turbines, whereas studies on floating wind turbines are limited. This research focus on the seismic vulnerability assessment of a 10 MW Tension Leg Platform Wind Turbine (TLP) developed by the Korean Institute of Energy Research (KIER). The fully coupled three-dimensional model of the Soil-Pile-Tension Leg Platform system is developed in Abaqus, accounting for both kinematic and inertial interactions. The soil is modelled as a 3D continuum with the Mohr-Coulomb constitutive model. Seismic demand is estimated for both serviceability and ultimate limit states using Peak Ground Acceleration (PGA) as the intensity measure. The study observed that TLP floating wind turbines are more vulnerable to near field seismic records as compared to far field earthquake. The critical mode of failure for TLPs are observed to be amplification of acceleration at nacelle primarily due to the vertical earthquake shaking. The variability of response at a particular intensity measure is observed to be higher due to the inherent uncertainty of seismic records and therefore it is recommended to consider a confidence interval for the design of TLP floating wind turbines. This study aims to identify potential seismic risks and provide guidelines for designing seismically resilient floating offshore wind structures.

Keywords: Tension leg platform, vulnerability, wind-wave, multi-directional earthquake, fragility

1 INTRODUCTION

The increasing global demand for renewable energy has driven significant advancements in offshore wind power generation, with floating offshore wind turbines emerging as a promising solution for harnessing wind energy in deeper waters. Among various floating platforms, tension leg platforms (TLPs) offer significant advantages, including high stability, minimal horizontal displacement, and cost-effectiveness compared to other designs (Butterfield et al., 2007). Tension Leg Platforms are particularly advantageous for large-scale offshore wind energy installations in intermediate water depths, owing to their efficient mooring configurations and inherent structural resilience under harsh marine conditions.

The expansion of offshore wind energy into earthquake prone areas underscores the imperative for advanced seismic structural design methodologies. Previous research has demonstrated the vulnerability of offshore wind turbines (OWTs) to seismic activity. De Risi et al. (2018) demonstrated the vulnerability of OWTs to crustal earthquakes, emphasizing the need for improved seismic resilience. Mo et al. (2021) investigated the impact of ground motion direction on the seismic dynamic responses of monopile-supported offshore wind turbines (OWT). The findings suggest that employing standard input in the fore-aft (FA) and side-to-side (SS) orientations may lead to an underestimation of the maximum structural dynamic responses. James and Haldar (2022, 2021) assessed the seismic sensitivity of jacket-supported wind turbines. Their analysis revealed a noticeable amplification of nacelle acceleration due to vertical earthquake shaking, underscoring the importance of accounting for multi-directional effects in design considerations. Additionally, Bhattacharya et al. (2021) and Kaynia (2019) provide a comprehensive review of existing seismic design standards and the prevailing challenges associated with wind turbine seismic design.Their work highlights the need for continued advancements in engineering approaches to enhance the resilience of offshore wind structures in earthquake-prone regions.

Previous studies were primarily focused on fixed wind turbine structure, while limited studies were conducted on floating OWT. For instance, James and Haldar (2024) analyzed the seismic vulnerability of spar floating wind turbines, concluding that these systems exhibit high resilience to seismic shaking due to the catenary mooring configuration and the significant damping effect of surrounding water. In the oil and gas sector, Kawanishi et al. (1993) investigated the seismic response of tension leg platform (TLP) floating systems, demonstrating that vertical earthquake components can alter cable pretension, potentially compromising platform stability. Bhattacharya et al. (2021) further assessed the seismic performance of TLPs under mooring failure conditions, showing that seismic shaking can increase the risk of overturning failure. Kaynia et al. (2023) reported that that vertically propagating pressure waves in seawater, known as seaquakes, induced by vertical seabed motion, can result in the snap tension on the leeward mooring. Tsiapas et al. (2021) analysed the effect of liquefaction on the TLP floating anchors and concluded that anchors supporting TLPs are susceptible to pull-out failure due to the development of excess pore water pressure. However, this study did not consider the coupled dynamics of the platform and tower, emphasizing the need for further research on fully integrated seismic analysis of floating wind turbine systems. Moreover, the prior research has not accounts the uncertainity inherent in the ground motion records.

This study assesses the seismic vulnerability of a 10 MW TLP floating wind turbine, developed by the Korean Institute of Energy Research (KIER) (Madsen et al., 2020), under combined seismic and environmental loads. It examines the effects of near-field and far-field earthquakes, considering multi-directional seismic records. By employing probabilistic fragility assessments, the research aims to enhance seismic design practices for floating offshore wind turbine systems.

2 NUMERICAL MODELLING

A three-dimensional numerical model of the Soil-Pile-Tension Leg Platform (TLP) system was developed in ABAQUS CAE (2018) (Fig. 1). The model incorporates the Korean Institute of Energy Research (KIER) concept (Madsen et al., 2020) supporting the DTU 10 MW baseline wind turbine (Bak et al., 2013) deployed at a water depth of 70 m. The detailed platform and turbine properties are reported in Table 1 and Table 2 respectively. The soil profile consists of two layers: a soft upper stratum underlain by stiff clay, reflecting typical site conditions in Gujarat, India. The soil profile comprises two layers, with the uppermost layer characterized by a soft clay, succeeded by a layer of stiff clay demonstrating the realistic site characteristics typical of Gujarat, India as shown in Fig. 1b. The soil is modelled as a 3D continuum (C3D8R element) described by Mohr-Coulomb constitutive model. Infinite elements are placed at the boundaries to absorb outgoing waves and minimize radiation damping effects. The superstructure including tower, platform are modelled as a beam element, while, the piles are modelled as solid element by providing equivalent stiffness. The truss elements modified with compression cut off are provided for modelling the tendons. The Rotor-Nacelle Assembly (RNA) is modelled as a lumped mass. The water is modelled by providing hydrostatic springs and viscous dampers. Assuming the platform to be a rigid body, the hydrostatic stiffness has been defined by the water plane area (A_{wp}), the overall centre of gravity (Z_G) and the centre of buoyancy (Z_B) from the water level. The stiffness is estimated by using the equations (1) and (2) (Bachynski & Moan, 2012),where V is the displaced water volume, and $\mathrm{I_{wp}}$ is the moment of inertia of the water plane area about pitch (for $\mathrm{K_{44}}$) and roll axis (for $\mathrm{K_{55}}$). The damping coefficient are directly taken from Madsen et al. (2022).

$$K_{33} = \rho g A_{wp} \tag{1}$$

$$K_{44} = K_{55} = \rho g I_{wp} + \rho g V Z_B - M g Z_G \tag{2}$$

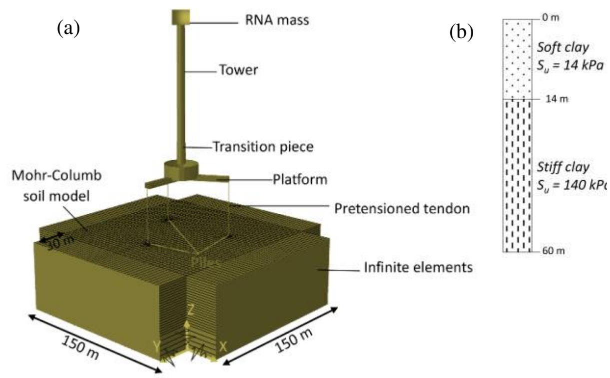

Figure 1. (a) Numerical model of TLP floating wind turbine developed in Abaqus CAE (b) Soil profile considered in this study

TLP stability relies on excess buoyancy thereby generating the tendon pretension. Static pretension is established by defining gravity and buoyant loads in the initial static step. The stability of TLP is maintained through excess buoyancy, which counteracts the gravity load to generate pretension in the tendon. Initially, the gravity and buoyant load is defined in the static step to establish the static pretension. Further, a free decay analysis is conducted to measure the natural period, which aligns closely with values reported in the literature (Madsen et al., 2020), as shown in Table 3. Environmental loads are applied during static and dynamic implicit steps. Seismic excitation is introduced at the soil domain base in all three directions (X, Y, Z) as a boundary condition. The soil base is fixed during the static step and subsequently released for seismic loading.

Table 1. Dimensions of 10MW TLP (KIER) platform

Property -10MW KIER	Dimension
Span length	60 m
Pontoon (B×H)	6 m × 8 m (root)
Central column dimension (D, H)	30 m
Height of transition piece	18 m
Water depth	70 m
Draft	19 m
Tendon length and diameter	132 mm

Table 2. Properties of the DTU 10 MW (Bak et al., 2013) reference wind turbine

Property	Value
Rating	10 MW (DTU)
Rotor Orientation	Upwind, 3 blades
Hub height	119 m
Rotor, hub diameter	178.3 m, 5.6 m
Cut-in, rated, cut-out speed	4 m/s, 11.4 m/s, 25 m/s
Cut-in, rated rotor speed	6.0 rpm, 9.6 rpm
Rated tip speed	90 m/s
RNA mass	676.7 ton
Tower Mass	605 ton

Table 3. Validation of the 10 MW TLP turbine model (Madsen et al., 2020) developed in Abaqus

Direction	10MW-TLP (KIER)	
	Numerical Model (sec)	**Reported** (Madsen et al., 2020)
Surge/Sway	32.31	32.27
Pitch/roll	3.772	3.77
heave	1.305	1.3

3 LOADING PARAMETERS AND GROUND MOTION RECORDS

The seismic analysis of TLP floating wind turbines is carried out under normal operation by assuming the turbine is operating under rated wind speed. Site- far-specific environmental parameters, detailed in Table 4, correspond to a proposed floating wind turbine location along India's west coast (James and Haldar, 2024). Strong ground motion records, sourced from the Pacific Earthquake Engineering Research Center (PEER) database, include both near-field and far-field events. Near-field motions are defined by a rupture distance within 20 km from the km from the fault (Veggalam et al., 2021). The selection comprises pulse and non pulse motions with varied spectral shapes across a wide range of periods and magnitudes (M 4.9–M 7.6). To ensure relevance with the soil taken for this study, shear wave velocities were chosen to represent soft to stiff clay layers. Table 5 summarizes the key properties of the selected ground motions.

Table 4. Environmental loading parameters used in this study

Loading parameters	Normal Operation
Wind Speed at hub	11.4 m/s
Wave Height (H_s)	4.1 m
Wave Period	10 sec
Current Velocity	0.3 m/s

4 SEISMIC RESPONSE OF TLP FLOATING WIND TURBINES

The seismic response of tension leg platform floating wind turbine to a typical earthquake motion is shown in Figure 2. To examine the effect of earthquake, only seismic load is considered without accounting for the environmental loading condition. A near field earthquake motion - Whittier Narrows 1987 scaled to a PGA of 0.5g is applied in three direction (H1, H2 and V) in this case. The acceleration response at nacelle is quite small as compared to the input acceleration, which is mainly due to the low stiffness and large natural period of the TLP in surge, sway direction, the horizontal motion is not getting transferred into the floating platform. However, the vertical component is getting amplified and which makes the vertical component of earthquake most vulnerable. The pretension response (P) at the tendon normalised with initial static pretension (P_s)is shown in Figure 2 (d). It is observed that the vertical earthquake component alters the pretension of the tendon. Therefore, the acceleration amplification, and the change in pretension at the tendon is observed as the most critical failure mode for TLP.

The seismic demand is evaluated through engineering demand parameters (EDPs), including nacelle acceleration (Fig. 3a), anchor pull-out failure (Fig. 3b), and tendon slack (Fig. 3c). Slacking of tendon is the condition at which the tendon pretension reduces to zero, which can affect platform stability and potentially lead to overturning. All responses are represented in terms of capacity factor except the tendon slack (Fig. 3c), which is expressed as the ratio of minimum pretension to the initial static pretension. The capacity factor is defined as the ratio of maximum demand during an earthquake to its permissible limit, with values exceeding one indicating a response beyond the allowable threshold (marked by a blue dotted line in the Fig. 3).

It is observed near-field earthquakes induce higher responses compared to far-field motions, primarily due to the presence of long-period velocity pulses. The pulse motion is characterized by high-amplitude velocity pulses, which transfer large kinetic energy over a short duration. This abrupt energy transfer leads to a rapid and severe structural response, increasing the risk of sudden failure. Additionally, the strong vertical components of near-field motions substantially influence seismic demands. The mean response for near-field motions consistently exceeds that of far-field motions, with the variation becoming more pronounced at higher PGA levels. Among the EDPs, nacelle acceleration is identified as the most critical parameter, exhibiting the highest probability of exceeding failure thresholds during seismic events. Significant variability in responses is observed within the same intensity level (PGA), likely due to inherent uncertainties in seismic records. This emphasizes the need to identify alternative Intensity Measures (IMs) and incorporate probailitstic fragility assessment with confidence intervals to ensure robust and reliable design practices.

5 FRAGILTY ANALYSIS

Seismic fragility refers to the probability of exceeding a certain damage state at a particular intensity of seismic motion (Porter et al., 2007). Fragility functions can be generated through several methods, including analytical, empirical, and hybrid approaches. The analytical method is the predominant strategy employed in the field of offshore wind turbines (OWTs) to assess the seismic risk of structures. An appropriate selection of intensity measure (IM) is needed to assess the seismic probabilities. Here, incremental dynamic analysis is performed by multiple nonlinear time history studies by varying the peak ground acceleration from 0.1g to 2g for the chosen set of earthquake events. Assuming a logarithmic relationship between both the engineering demand parameters (EDP) and intensity measure (IM), fragility of offshore wind turbines (OWT) can be defined by equation 3 (Baker 2015):

$$[EDP > ds_i \,|PGA] = \Phi\left[\frac{\ln(PGA/\xi)}{\sigma}\right] \qquad (3)$$

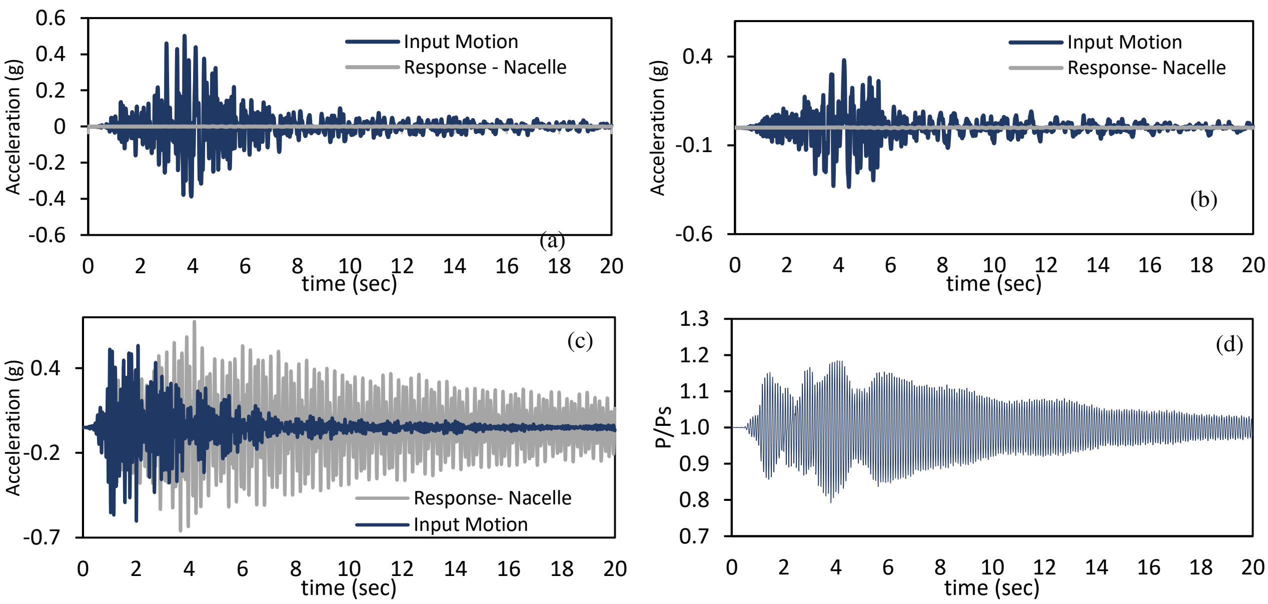

Figure 2. The seismic response of TLP floating wind turbines to a typical earthquake motion (a) acceleration at nacelle- horizontal component1 (b) horizontal component 2(c) vertical component (d) pretension at the tendon normalised with the initial static pretension

Table 5. Properties of selected strong ground motions (PEER, 2013)

Sl. No	Earthquake Name	Year	Type	Magnitude	$V_{s,\,30}$	V/H
1	Humbolt Bay	1937	Far Field	5.8	219.31	0.37
2	Whittier Narrows	1987	Far Field	5.99	160.58	0.41
3	Coalinga	1983	Far Field	6.36	212	0.29
4	Northwest-California	1941	Far Field	6.6	219.31	0.31
5	Chi-Chi Taiwan	1999	Far Field	7	297.86	0.46
6	Darfield, New Zealand	2010	Far Field	7	211	0.7
7	Landers	1992	Far Field	7.28	353.63	0.55
8	Taiwan Smart	1986	Far Field	7.3	285	0.26
9	Anza	2001	Far Field	4.92	196	0.24
10	Kocaeli	1999	Near Field	7.51	297	0.76
11	Chi-Chi Taiwan	1999	Near Field	7.62	258.89	0.50
12	Central-Calif-02	1960	Near Field	5	198.77	0.40
14	Whittier Narrows	1987	Near Field	5.99	160.58	1.26
15	Northwest China	1997	Near Field	6.1	240	1.3
16	Superstition Hills-01	1987	Near Field	6.22	179	1.4
17	Imperial valley	1979	Near Field	6.53	203.22	4.2
18	Irpinia Italy	1980	Near Field	6.9	203.22	0.83
19	Kobe Japan	1995	Near Field	6.9	198	1.6
20	Loma Prieta	1989	Near Field	6.93	270.84	0.8

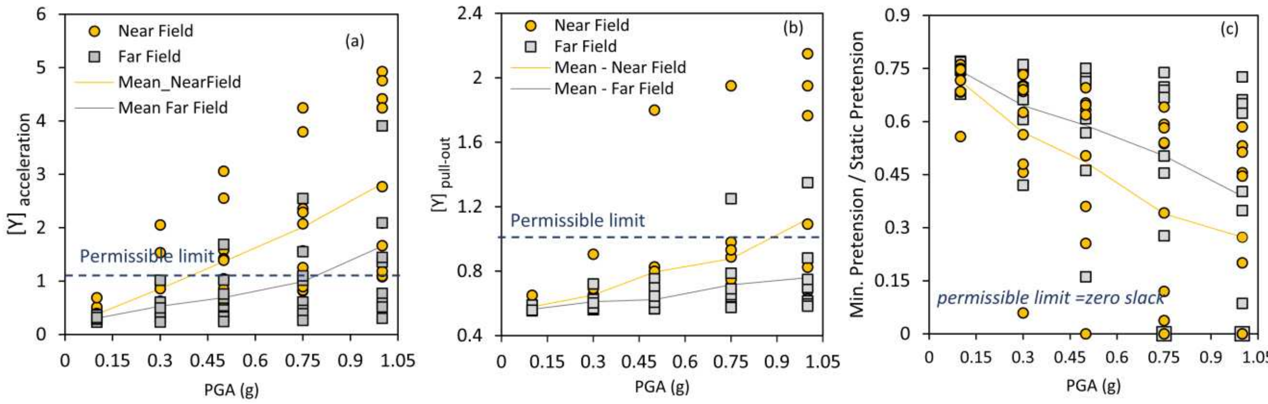

Figure 3. The seismic response of TLP floating wind turbines to near field and far field motion (a) acceleration at nacelle (b) pull-out failure in anchor (c) minimum pretension at the tendon

Where, $\Phi(.)$ is the standard normal distribution function; ξ and σ refers to the median and standard deviation of the fragility function. The likelihood of damage is evaluated according to a single damage state, characterized by limit state requirements. Among several engineering demand parameters, the acceleration at the nacelle, tendon slack, pull-out failure in the anchor, and yielding of the tower are regarded as the most relevant damage state to fully assess the damage level in TLP floating wind turbines.

While estimating a fragility curve, there is inherent uncertainty due to limitations in data, model assumptions, and variability in the response of structures to hazards. Additionally, the likelihood for the variation within the same intensity is very high which is noticeable from Fig. 3. To address this, a 95% confidence interval is incorporated into the fragility curve. This interval quantifies the range within which the true fragility curve is expected to lie with 95% confidence, assuming the statistical model is accurate.

The developed fragility curve with a 95% confidence interval is presented in Fig. 4. Except for the nacelle acceleration, the failure probability for other responses remains below 1, even under a peak ground acceleration (PGA) of 2g. This resilience is attributed to the high tendon pretension, which enhances system stability. However, nacelle acceleration exhibits a significantly higher failure probability, reaching 0.8 at a PGA of 1g, primarily due

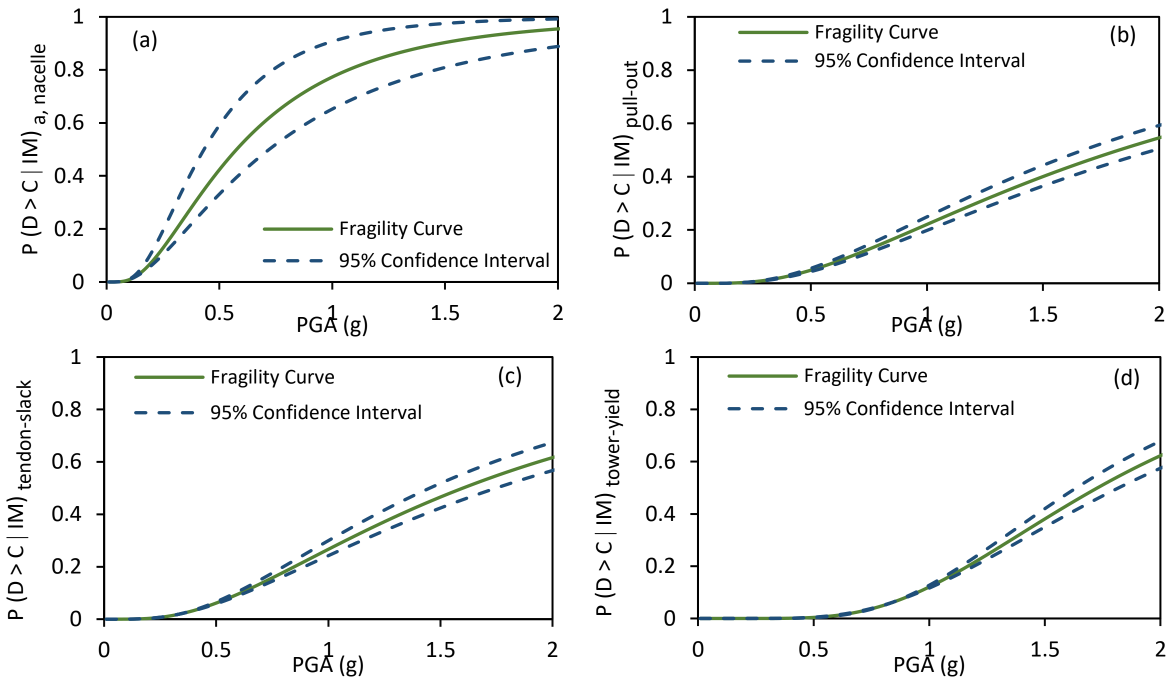

Figure 4. Fragility curves for TLP floating wind turbines with 95% confidence interval (a) acceleration at nacelle (b) pull-out failure in anchor (c) tendon slack (d) yield failure in tower

Table 6. Defining damage states in SLS and ULS criteria for OWT

Limit states	**Damage measures (DM)**	**Damage states (DS)**
SLS	Nacelle acceleration	0.6 g (Cheng et al., 2023)
	Slack in tendon	Zero pretension
ULS	Pull-out Failure of Anchor (Tsiapas et al., 2021)	Uplift capacity = 2 × the static pretension
	Von Mises stress tower (Jay et al., 2016)	266 MPa

to the vertical component of earthquake. This is attributed to the large acceleration amplification at the nacelle, driven by the resonance caused by the proximity of the earthquake's predominant vertical frequency to the heave natural frequency. To mitigate this, damping devices such as liquid column dampers, tuned mass dampers, viscous dampers, or magnetorheological tuned vibration absorbers are recommended. With appropriate modifications, tension leg platforms (TLPs) could serve as a viable alternative for offshore wind energy in seismically active regions, offering greater resilience to seismic events compared to fixed offshore wind turbines.

6 CONCLUSIONS

This study investigates the seismic vulnerability of a 10 MW KIER Tension Leg Platform (TLP) floating wind turbine under multi-directional seismic shaking. The analysis includes a detailed assessment of near-field and far-field earthquake motions, considering uncertainties using a large earthquake data scaled to PGAs ranging from 0.1g to 2g, characterised with a varied spectral shape across a wide range of periods and magnitudes to analyse the vulnerability. Initially a comparison between near filed and far field earthquake motion is carried out. Further, fragility curves are suggested with 95% confidence interval. Results indicate that near-field earthquake motions pose greater vulnerability compared to far-field motions, primarily due to large velocity pulses. A significant variation between responses is observed within the same intensity level outlining the necessity to search for more efficient intensity measures. The vertical component of earthquakes is observed to be particularly critical, as it amplifies nacelle acceleration and alters mooring pretension. Among the EDPs, nacelle acceleration is identified as the most critical, exhibiting the highest probability of exceeding failure thresholds. To address this, the use of damping devices, such as liquid column dampers, tuned mass dampers, viscous dampers, or magneto rheological tuned vibration absorbers, is recommended. In contrast, failure probabilities for other responses such as yielding of tower, the tendon slack, and pull-out failure remain below 60% even at a very high PGA of 2g. This is mainly due to the high tendon pretension, which enhances system stability. Therefore, with proper modifications, TLPs demonstrate potential as a resilient alternative for offshore wind energy in seismically active regions, offering advantages over fixed offshore wind turbines.

AUTHORS CONTRIBUTION STATEMENT

First Author: conceptualization, developed the methodology, conducted the analysis, and drafted the original manuscript**. Second Author and Third Author**: conceptualization, supervised the research, provided critical feedback, and contributed to the interpretation of results and revision of the manuscript.

REFRENCES

Bachynski, E. E., & Moan, T. (2012). Design considerations for tension leg platform wind turbines. *Marine Structures*, *29*(1), 89-114.

Bak, C., Zahle, F., Bitsche, R., Kim, T., Yde, A., Henriksen, L. C., ... and Hansen, M. (2013). Description of the DTU 10 MW reference wind turbine. *DTU Wind Energy Report-I-0092*, *5*.

Baker, J. W. (2015). Efficient analytical fragility function fitting using dynamic structural analysis. *Earthquake Spectra*, *31*(1), 579-599.

Bhattacharya, S., De Risi, R., Lombardi, D., Ali, A., Demirci, H. E., and Haldar, S. (2021). On the seismic analysis and design of offshore wind turbines. *Soil Dynamics and Earthquake Engineering*, *145*, 106692.

Bhattacharya, S., Biswal, S., Aleem, M., Amani, S., Prabhakaran, A., Prakhya, G., ... and Mistry, H. K. (2021). Seismic design of offshore wind turbines: good, bad and unknowns. *Energies*, *14*(12), 3496.

Butterfield, S., Musial, W., Jonkman, J., and Sclavounos, P. (2007). Engineering challenges for floating offshore wind turbines (No. NREL/CP-500-38776). *National Renewable Energy Lab.*(NREL), Golden, CO (United States).

Cheng, Y., Luo, Y., Wang, J., Dai, K., Wang, W., and El Damatty, A. (2023). Fragility and vulnerability development of offshore wind turbines under aero-hydro loadings. *Engineering Structures*, *293*, 116625.

Dassault Systèmes. (2018). *Abaqus 2018 Documentation*. Dassault Systèmes Simulia Corp. https://www.3ds.com/productsservices/simulia/products/abaqus/

De Risi, R., Bhattacharya, S., and Goda, K. (2018). Seismic performance assessment of monopile-supported offshore wind turbines using unscaled natural earthquake records. *Soil Dynamics and Earthquake Engineering*, *109*, 154-172.

James, M. and Haldar, S. (2022) Seismic Vulnerability of Jacket Supported large Offshore Wind Turbine Considering Multi-Directional Ground Motions. Structures. 43:407-423.

James, M., Haldar, S., and Bhattacharya, S. (2022, December). Seismic Response of Spar Floating Offshore Wind Turbine. In *Indian Geotechnical Conference* (pp. 331-341). Singapore: Springer Nature Singapore.

James, M. and Haldar, S. (2021). Seismic design of large offshore wind turbine considering rocking vibration. In Transportation, Water and Environmental Geotechnics: *Proceedings of Indian Geotechnical Conference 2020* Volume 4 (pp. 411-422). Springer Singapore.

James, M. and Haldar, S. (2024). Design Strategies of Offshore Wind Turbines in Shallow and Deep Water-Indian Perspective. Indian Geotechnical Journal, 1-16.

Jay, A., Myers, A. T., Torabian, S., Mahmoud, A., Smith, E., Agbayani, N., and Schafer, B. W. (2016). Spirally welded steel wind towers: Buckling experiments, analyses, and research needs. *Journal of Constructional Steel Research*, *125*, 218-226.

Kawanishi, T., Ohashi, S., Takamura, H., and Kobayashi, H. (1993, June). Earthquake response of the tension leg platform under unbalanced initial tension. In *ISOPE International Ocean and Polar Engineering Conference* (pp. ISOPE-I). ISOPE.

Kaynia, A.M. (2019) Seismic considerations in design of offshore wind turbines. Soil Dyn Earthq Eng; 124:399–407.

Kaynia, A. M., Blekastad, H., Schell, P., & Walter, E. L. (2023). Seismic response of floating wind turbines due to seaquakes. *Wind Energy*, *26*(2), 145-162.

Madsen, F. J., Nielsen, T. R. L., Kim, T., Bredmose, H., Pegalajar-Jurado, A., Mikkelsen, R. F., ... and Shin, P. (2020). Experimental analysis of the scaled DTU10MW TLP floating wind turbine with different control strategies. *Renewable Energy*, *155*, 330-346.

Mo, R., Cao, R., Liu, M., and Li, M. (2021). Effect of ground motion directionality on seismic dynamic responses of monopile offshore wind turbines. *Renewable Energy*, *175*, 179-199

Pacific Earthquake Engineering Research Center. (PEER). (2013). *PEER Ground Motion Database*.

University of California, Berkeley. Retrieved from https://ngawest2.berkeley.edu/

Porter, K., Hamburger, R., & Kennedy, R. (2007). Practical development and application of fragility functions. In *Structural engineering research frontiers* (pp. 1-16).

Tsiapas, Y. Z., Chaloulos, Y. K., Bouckovalas, G. D., and Bazaios, K. N. (2021). Performance based design of Tension Leg Platforms under seismic loading and seabed liquefaction: A feasibility study. *Soil Dynamics and Earthquake Engineering*, *150*, 106894.

Veggalam, S., Reddy, K. K., and Somala, S. N. (2021, December). Collapse fragility due to near-field directivity ground motions: Influence of component, rupture distance, hypocenter location. In *Structures* (Vol. 34, pp. 3684-3702). Elsevier.